

Original Research

# Exosomal CircRNAs in Circulation Serve as Diagnostic Biomarkers for Acute Myocardial Infarction

Xiaoyan Liu<sup>1,2,3,†</sup> , Yeping Zhang<sup>1,2,†</sup>, Wen Yuan<sup>3</sup>, Ruijuan Han<sup>4</sup>, Jiuchang Zhong<sup>1,2</sup>,  
Xinchun Yang<sup>1,2,\*</sup>, Meili Zheng<sup>1,2,\*</sup>, Boqia Xie<sup>1,2,5,\*</sup><sup>1</sup>Heart Center and Beijing Key Laboratory of Hypertension, Beijing Chao-Yang Hospital, Capital Medical University, 100020 Beijing, China<sup>2</sup>Department of Cardiology, Beijing Chao-Yang Hospital, Capital Medical University, 100020 Beijing, China<sup>3</sup>Medical Research Center, Beijing Institute of Respiratory Medicine and Beijing Chao-Yang Hospital, Capital Medical University, 100020 Beijing, China<sup>4</sup>Department of Cardiology, The Second Affiliated Hospital, School of Medicine, The Chinese University of Hong Kong, Shenzhen & Longgang District People's Hospital of Shenzhen, 518172 Shenzhen, Guangdong, China<sup>5</sup>Department of Cardiac Surgery, Beijing Chaoyang Hospital, Capital Medical University, 100020 Beijing, China\*Correspondence: [15896053808@163.com](mailto:15896053808@163.com) (Xinchun Yang); [zhengmeilicyh@mail.ccmu.edu.cn](mailto:zhengmeilicyh@mail.ccmu.edu.cn) (Meili Zheng);[dr.boqiaxie@mail.ccmu.edu.cn](mailto:dr.boqiaxie@mail.ccmu.edu.cn) (Boqia Xie)

†These authors contributed equally.

Academic Editor: Rajesh Katare

Submitted: 18 November 2023 Revised: 6 February 2024 Accepted: 21 February 2024 Published: 11 April 2024

## Abstract

**Background:** The diagnostic potential of circular RNAs (circRNAs) in circulating exosomes for acute myocardial infarction (AMI) is not well understood, despite existing research indicating their role in cardiovascular diseases. This study aimed to clarify the significance of exosomal circular RNAs as indicators for AMI. **Methods:** We examined 120 individuals diagnosed with AMI and 83 individuals with non-cardiogenic chest pain (NCCP), all previously enrolled in a conducted study. High-throughput sequencing to identify differentially expressed circRNAs in the circulating exosomes of AMI patients. To validate, we employed Real-Time polymerase chain reaction (RT-PCR) targeting five circRNAs that exhibited notable increase. **Results:** The sequencing identified 893 exosomal circRNAs with altered expression in AMI patients, including 118 up-regulated and 775 down-regulated circRNAs. Genes linked to these circRNAs were enriched in crucial Kyoto Encyclopedia of Genes and Genomes (KEGG) pathways, highlighting their direct relevance to AMI pathophysiology. Three exosomal circRNAs (hsa\_circ\_0001558, hsa\_circ\_0001535, and hsa\_circ\_0000972) showed significant up-regulation in AMI patients during the initial validation cohort. The corresponding area under the curve (AUC) values were 0.79, 0.685, and 0.683, respectively. Further validation of hsa\_circ\_0001558 in a second cohort showed a 4.45-fold increase in AMI patients, with AUC = 0.793. The rise was particularly noticeable in patients with non-ST-elevation myocardial infarction (NSTEMI) (2.80 times, AUC = 0.72) and patients with ST-elevation myocardial infarction (STEMI) (5.27 times, AUC = 0.831) compared to patients with NCCP. **Conclusions:** Our findings demonstrate significant differences in the expression patterns of circRNAs in plasma exosomes between AMI patients and NCCP patients. Specifically, hsa\_circ\_0001558 appears as a promising indicator for AMI diagnosis. Further research is necessary to fully evaluate the diagnostic potential of exosomal circRNAs in the context of AMI, emphasizing the importance of these findings.

**Keywords:** acute myocardial infarction; exosome; circRNA; biomarkers

## 1. Introduction

Cardiovascular diseases, particularly Acute Myocardial Infarction (AMI), remain a major contributor to worldwide illness and death [1]. Despite progress in medical science, promptly and accurately diagnosing AMI poses a significant challenge. Current diagnostic approaches, including cardiac biomarkers, electrocardiography, and imaging techniques, provide useful information but frequently lack the precision needed for timely and precise diagnosis [2,3]. As a result, there is a continuous effort to discover new biomarkers that can improve AMI diagnosis, allowing for swift intervention and better patient outcomes [4].

In recent years, there has been a growing interest in the potential role of exosomal circular RNAs (circRNAs) as

diagnostic markers in cardiovascular diagnostics [5]. CircRNAs, characterized by their circular structure, are transported by exosomes—tiny vesicles released by various cell types [6]. Closed-loop structured circRNAs have demonstrated regulatory roles in diverse biological processes and have been linked to multiple diseases [7–9]. Exosomes are now recognized as significant contributors to cardiovascular health and disease, influencing angiogenesis and cardiomyocyte function, crucial elements in cardiovascular disease pathogenesis. Understanding the effects mediated by exosomes and associated biomarkers is crucial for managing cardiovascular diseases, including myocardial infarction (MI) [10]. Research by Li *et al.* [11] indicated the active transfer of circRNAs from cells to exosomes and



underscores the potential of circRNAs to serve as disease biomarkers [11]. However, the current understanding of the presence of circRNA in exosomes circulating among patients with AMI and its potential as a diagnostic indicator remains uncertain.

In this study, a meticulous approach is employed, incorporating high-throughput sequencing, real-time polymerase chain reaction (RT-PCR), and diverse analytical methods to identify and validate specific exosomal circRNAs with potential as biomarkers for AMI. These methods enable the assessment of the diagnostic accuracy of exosomal circRNAs, laying the groundwork for their potential clinical application.

## 2. Materials and Methods

### 2.1 Patients

In this study, we enrolled a total of 203 participants from our prior investigation [12], categorized into three cohorts. The initial group, designated as the sequencing group, encompassed 15 individuals diagnosed with acute myocardial infarction (AMI) and 15 individuals with non-cardiac chest pain (NCCP). The first validation cohort, included 20 AMI patients and 20 NCCP patients. The second validation cohort, comprised 85 AMI patients and 48 NCCP patients. The research adhered to the guidelines outlined in the Declaration of Helsinki and received approval from the Ethics Committee of Beijing Chao-Yang Hospital (2016-ke-101). All participants provided consent after receiving pertinent information.

Participants in this study were selected based on strict inclusion and exclusion criteria to ensure the integrity of our findings. For inclusion, AMI patients were identified through clinical symptoms, specific electrocardiogram (ECG) changes, and elevated cardiac biomarkers, namely troponin-I (TnI) and creatine kinase MB (CKMB), following the Universal Definition of Myocardial Infarction. NCCP controls included individuals with chest pain but normal cardiac biomarkers and no coronary stenosis, as confirmed by angiography. Exclusion criteria were applied rigorously to minimize confounding factors, excluding individuals with malignant diseases, severe organ failure (renal, hepatic, or heart failure), thyroid dysfunction, autoimmune diseases, acute or chronic infectious diseases, and pregnant women.

### 2.2 Sample Collection

We employed standard venipuncture techniques to collect fasting venous blood samples from all participants. Subsequently, the obtained blood underwent processing for plasma extraction through centrifugation at 4 °C for 10 minutes at 3000 RPM. Following meticulous separation, the plasma samples were partitioned into smaller aliquots and preserved at a temperature of –80 °C until subsequent analysis.

### 2.3 Exosome Isolation

Plasma-derived exosomes were acquired using the exoEasy Maxi kit (Qiagen, Hilden, Germany, 76064), following the producer's instructions. In brief, plasma previously frozen at –80 °C was thawed at 37 °C and then subjected to centrifugation at 10,000 g for 15 minutes to isolate the supernatant. This 4 mL supernatant was transferred to a new 15 mL centrifuge tube. Subsequently, an equivalent volume of buffer was gently mixed with the plasma, and the mixture was incubated at room temperature. The blend was loaded into a column, centrifuged at 500 g for 1 minute, and the waste was discarded. The column was repositioned into the centrifuge tube. Next, 10 mL of buffer was added to the column, followed by centrifugation at 3000 g for 5 minutes. The column was then moved to a new centrifuge tube. Finally, 1 mL of elution solution was introduced to the column, incubated for 1 minute, and centrifuged at 500 g for 5 minutes. The filtered liquid was collected, reintroduced to the column for an additional 60 seconds, and subsequently subjected to centrifugation at a force of 500 g for 5 minutes. The resulting filtrate was gathered in a fresh eppendorf tube devoid of RNase and stored at –80 °C for future use.

### 2.4 Exosome Size Analysis

For exosome size analysis, 1 mL of phosphate-buffered saline (PBS) was added to the exosome suspension and thoroughly mixed. Measurement was performed using the Zeta View-Particle Metrix nanoparticle tracking analysis instrument (ZetaView 8.04.02, Particle Metrix GmbH, Meerbusch, North Rhine-Westphalia, Germany). The sample was introduced into the sample chamber, and the software was initiated. Adjustments were made for brightness and focus, and the field of view was set for observation. The software then analyzed particle size by tracking the time and displacement of the particle's motion trajectory.

### 2.5 Transmission Electron Microscopy (TEM) Analysis of Exosomes

For transmission electron microscopy (TEM) analysis of exosomes, the isolated exosomes underwent treatment with a 2% paraformaldehyde solution (P0099, Beyotime, Beijing, China). A small volume of the exosome solution was then applied to a Formvar-carbon-coated copper grid and allowed to incubate for 10 minutes at room temperature. The grid was rinsed with phosphate-buffered saline (PBS) solution and subsequently treated with a 1% glutaraldehyde solution (G6257, Merck, Darmstadt, Germany), followed by rinsing with distilled water. Afterward, the grid underwent treatment with uranyl acetate solution (U25690, Acmecc, Shanghai, China) and methyl cellulose solution (ST1510, Beyotime, Beijing, China) before being air-dried. Finally, the copper grid was positioned in a sample holder and imaged using TEM (JEM-2100, JEOL Ltd., Tokyo, Japan) at 80 kV, with appropriate adjustments made to focus and brightness settings.

## 2.6 Western Blotting

For Western blotting, the supernatant was mixed with 1/5 of 5× loading buffer and heated for 5 minutes. Subsequently, a 20 µL sample was loaded onto a 10% SDS-polyacrylamide gel for electrophoresis. After transferring the proteins onto a polyvinylidene fluoride (PVDF) membrane (3010040001, Merck KGaA, Darmstadt, Germany), they were blocked with 5% bovine serum albumin (BSA) (ST023, Beyotime, Beijing, China) for 1 hour. The membrane was then incubated overnight at 4 °C with antibodies specifically cluster of differentiation 63 (CD63) antibody (ab68418, 1:1000, abcam, Cambridge, MA, USA), heat shock protein 70 (HSP70) antibody (ab2787, 1:3000, abcam, Cambridge, MA, USA), or GAPDH antibody (ab9485, 1:5000, abcam, Cambridge, MA, USA). Following a TBST wash, the membrane was exposed to a 1:15,000 dilution of either anti-rabbit (92632211, LI-COR Biosciences, Lincoln, NE, USA) or anti-mouse secondary antibody (92632210, LI-COR Biosciences, Lincoln, NE, USA) and incubated for 1 hour at room temperature. After additional washes, the membrane was exposed for detection.

## 2.7 Extraction of Total RNA from Exosomes

Total RNA from exosomes was extracted using the exosome RNA extraction kit (217184, Qiagen, Hilden, Germany). The exosome solution was mixed with lysis buffer, and after centrifugation, the supernatant was collected. Chloroform was added to separate the aqueous phase, which was then combined with ethanol. This mixture was applied to columns provided in the kit, subjected to centrifugation, and washed. The columns were transferred to new tubes, and the filter membranes were dried. Elution buffer was introduced, and after centrifugation, the columns were discarded. The filtrate was then collected and stored at −80 °C. The RNA concentration was determined using NanoDrop 2000 (Thermo Fisher Scientific, Waltham, MA, USA), which measured the quantity of RNA, its concentration, and the absorbance ratio at 260/280.

## 2.8 High-Throughput Sequencing

For sequencing profile generation, plasma samples from every 5 patients with AMI and every 5 patients with NCCP were amalgamated into one ‘sample’, leading to the creation of ‘3 AMI’ and ‘3 control’ samples for profiling. Initially, exosome RNA undergoes preliminary processing steps, including purification. Subsequently, cDNA is synthesized through reverse transcription, followed by end repair and adapter ligation to prepare the library. Once passing quality control, the libraries undergo sequencing.

## 2.9 Bioinformatics Analysis

After acquiring the raw sequencing data, the initial steps involve data filtering, adapter trimming, and processing of low-quality reads. This is followed by

an assessment of sequencing quality and removal of ribosomal RNA (rRNA) to ensure the generation of high-quality data, termed as Clean Data. The clean data is initially mapped using Tophat2 software (Version 2.1.1.1, <http://ccb.jhu.edu/software/tophat/index.shtml>) for a standard alignment, excluding gene fusions (unfusion). This process aims to identify reads that cannot be directly mapped to the genome (unmapped reads). Subsequently, Tophat2’s Tophat-fusion module is employed to align these unmapped reads for fusion gene (fusion) mapping, capturing potential circRNA-forming reads. CircRNAs are identified using Python software (Version 3.9, <https://www.python.org/>) based on their unique back-splicing junctions, where exon sequences are rearranged. Junction reads are detected and refined with Tophat-fusion, focusing on typical GT/AG splice sites for precise circRNA identification. The expression levels of circRNAs are determined based on the predicted circRNA sequences. This involves counting the circRNA-associated reads, including both TopHat mapping and TopHat-fusion mapping reads, and calculating their RPM (Reads Per Million mapped reads). The count value for each circRNA is calculated using HTseq software (Version 2.0.0, <https://htseq.readthedocs.io/en/latest/index.html>), which then determines its RPM value. To calculate RPM, the number of reads mapping to circRNA is divided by the total number of mapping reads and multiplied by 10<sup>6</sup>.

Based on RPM results, Audic’s method is used to calculate the *p*-values and *q*-values for genes in comparison groups. CircRNAs with a fold change ( $\log_2(\text{Fold change}) > 1$ ) and a significance level (*q*-value < 0.001) are selected to determine differential expression among samples. The overall distribution of differentially expressed circRNAs is represented using a Volcano Plot. Additionally, we analyzed genes associated with differentially expressed circRNA sequences within Kyoto Encyclopedia of Genes and Genomes (KEGG) pathways to understand their impact on biological processes. By examining these pathways, this analysis provides an indirect approach to investigating the possible functions of circRNAs, establishing a foundation for future studies on their functionality. The Fisher Exact Test was employed to determine the significance (*p* < 0.05) of these genes in KEGG pathways, identifying statistically significant signal transduction and disease pathways.

## 2.10 Real-Time PCR (RT-PCR)

The expression levels of exo-circRNAs were quantified using the ViiA 7 Real-Time PCR System (Applied Biosystems, Foster City, CA, USA). The relative fold-change was calculated using the 2<sup>−ΔΔCT</sup> method. The primer sequences employed for amplification are listed in Table 1.

**Table 1. Primer sequence information of RT-PCR.**

CircRNA ID	Primer Sequence
hsa_circ_0001535-Forward Primer	GAGACTGTTCAAAACCTGTGGC
hsa_circ_0001535-Reverse Primer	CTGTAGAGGCTGGTAGGATGCT
hsa_circ_0003270-Forward Primer	CATCATCTTCATCCCCGAGTAA
hsa_circ_0003270-Reverse Primer	TTACCACAGCAGAAGCCCCCT
hsa_circ_0000972-Forward Primer	TTGTGTTTGGCTCTGGGATACCT
hsa_circ_0000972-Reverse Primer	GCACACTACAAAGTTGACCCTGA
hsa_circ_0001119-Forward Primer	AAGCATTCTATCTTTCTCCCCG
hsa_circ_0001119-Reverse Primer	TGACGCTCTTCACCTCGTTGTA
hsa_circ_0001558-Forward Primer	GCCCCGCTATGTGACCAATG
hsa_circ_0001558-Reverse Primer	TGAAGCAGGTACAGAGTTTCCC
hsa-18S-Forward Primer	CGCTCGCTCCTCTCCTACTT
hsa-18S-Reverse Primer	CGGGTTGGTTTTGATCTGATAA

RT-PCR, Real-Time polymerase chain reaction; CircRNA, circular RNAs.

### 3. Results

#### 3.1 Study Design and Patients

Our previous study involved a total of 203 participants, distributed across three cohorts, as detailed earlier [12]. The sequencing group comprised 15 individuals diagnosed with acute myocardial infarction (AMI) and 15 individuals with non-cardiac chest pain (NCCP). This group aimed to investigate the profile of circulating exosomal circRNAs and identify potential candidate circRNAs through high-throughput sequencing. The first validation cohort included 20 AMI patients and 20 NCCP patients. Its primary objective was to validate the candidate exosomal circRNAs identified in the sequencing cohort using real-time PCR (RT-PCR). This cohort served as a small-scale validation. The second validation cohort comprised 85 AMI patients and 48 NCCP patients. The purpose of this cohort was to confirm the presence of exosomal circRNAs identified in the first validation cohort but on a larger scale. Fig. 1 illustrates the study flow and cohort distribution.

#### 3.2 Identification of Plasma Exosomes

Plasma exosomes were identified through Western blotting, nanoparticle tracking analysis (NTA), and transmission electron microscopy (TEM) following their isolation from blood samples. Western blotting revealed the presence of specific exosomal marker proteins CD63 and HSP70 in both groups (Fig. 2A). NTA indicated that the exosomes had a diameter of around 100 nm (Fig. 2B). TEM analysis illustrated the vesicular structure of exosomes, characterized by a circular, bilayer membrane (Fig. 2C). These findings are consistent with the typical features of exosomes.

#### 3.3 Sequencing Profiles of Circulating Exosomal CircRNA in AMI Patients

To investigate the profile of circRNA in plasma exosomes of individuals with AMI, we conducted a comprehensive sequencing analysis on samples from a group of 15

NCCP participants and another group of 15 AMI patients, referred to as the sequencing cohort. The baseline characteristics of the subjects used for sequencing are available in our previously published data [12]. No significant disparities in age and gender were observed between the AMI and NCCP cohorts. Consistent with the clinical features of AMI patients, levels of cTNT, CK-MB, and NT-proBNP were notably elevated in the AMI group compared to the NCCP group.

High-throughput sequencing revealed significant disparities in the expression profile of circRNAs in plasma exosomes of AMI patients compared to the control group. Based on the criteria of  $|\log_2(\text{Fold change})| > 1$  and  $q\text{-value} < 0.001$ , a total of 893 circRNAs with differential expression were identified in AMI plasma exosomes. Among these, 118 circRNAs were upregulated, while 775 circRNAs were downregulated (Fig. 3A).

#### 3.4 Pathway Analysis of Circulating Exosomal CircRNAs in AMI Patients

Studies have shown that some circRNAs function by regulating the linear transcripts of their corresponding genes [13,14], indicating a significant association between circRNAs and the functions of their corresponding genes. Therefore, we analyzed genes associated with differentially expressed circRNA sequences within specific KEGG pathways. KEGG categorizes these pathways into four separate groups: Cellular Processes, Environmental Information Processing, Human Diseases, and Organismal Systems. The analysis revealed that genes associated with these circRNAs were notably concentrated in focal adhesion (Cellular Processes), mammalian target of rapamycin (mTOR) signaling pathway (Environmental Information Processing), pathways in cancer (Human Diseases), and thyroid hormone signaling pathway (Organismal Systems) (Fig. 3B). This suggests a direct correlation between the varying expression of specific circRNAs and their influence on these crucial biological pathways.

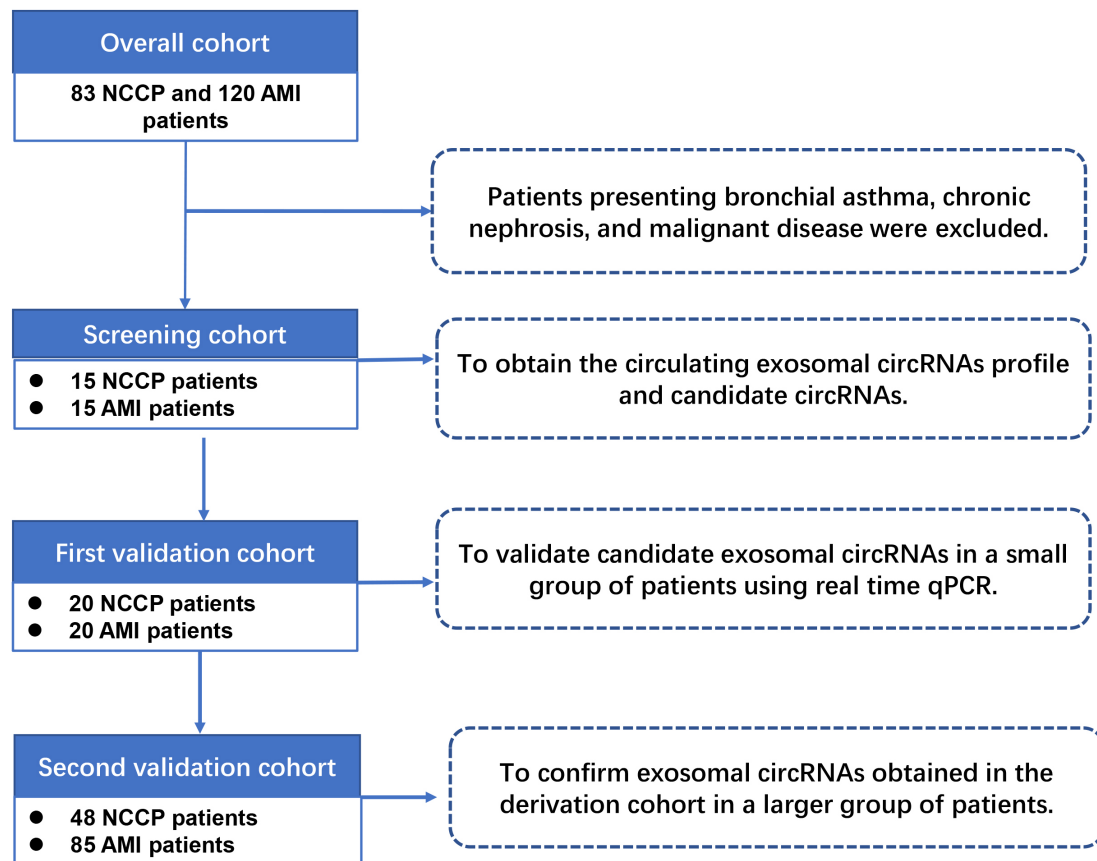


Fig. 1. Study flow diagram. AMI, acute myocardial infarction; NCCP, non-cardiogenic chest pain.

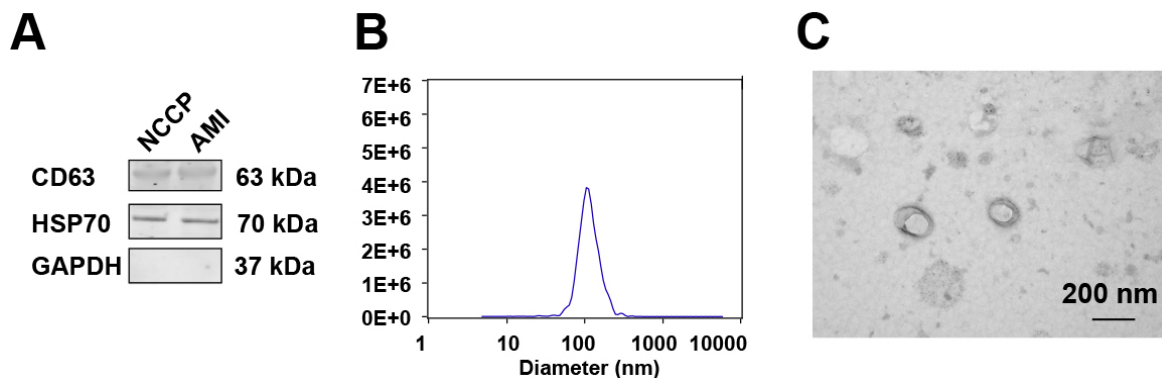


Fig. 2. Identification of plasma exosomes. (A) Western blotting results. (B) NTA results. (C) TEM results. HSP70, heat shock protein 70; AMI, acute myocardial infarction; NCCP, non-cardiogenic chest pain; NTA, nanoparticle tracking analysis; TEM, Transmission electron microscopy.

Among these differentially expressed circRNAs, 107 were annotated in circBase. To validate the results obtained through high-throughput sequencing and assess their potential as biomarkers, we selected five circRNAs that were upregulated according to the sequencing results. These circRNAs exhibited both high expression levels and substantial fold changes within the AMI group. Specifically, the selected circRNAs were: hsa\_circ\_0001535, hsa\_circ\_0003270, hsa\_circ\_0000972, hsa\_circ\_0001119,

and hsa\_circ\_0001558 (Fig. 3C). To validate these findings, we conducted RT-PCR experiments on a small set of specimens, comprising our first validation cohort.

### 3.5 The First Validation Cohort to Validate Candidate Exosomal CircRNAs

The RT-PCR validation results revealed that hsa\_circ\_0001119 consistently displayed a low and undetectable expression level in the majority of samples. Additionally, there was no significant difference

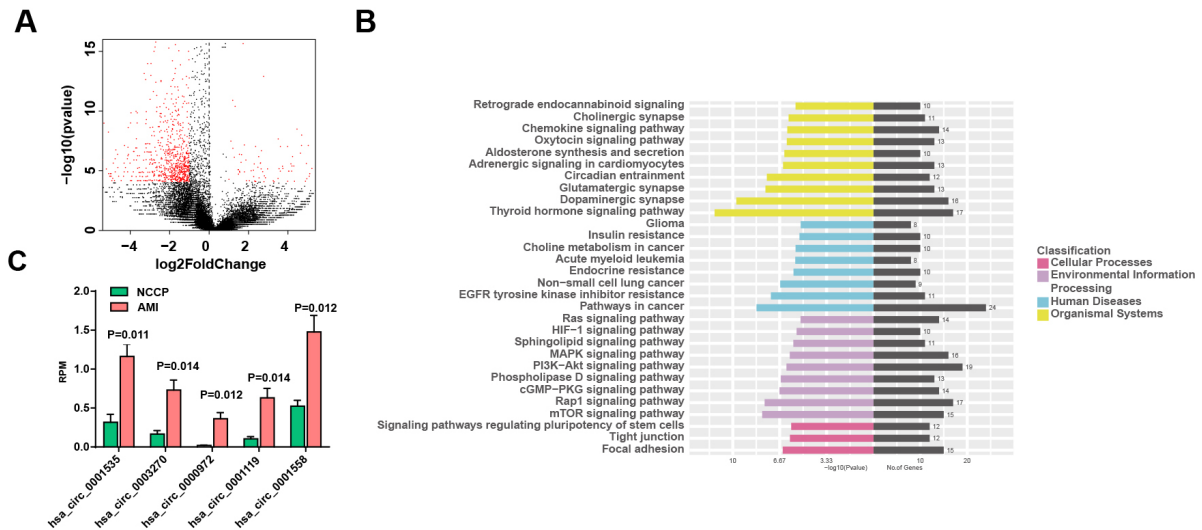


**Fig. 3. Differential expression and pathway analysis of circulating exosomal circRNAs in AMI patients.** (A) Volcano plot displaying the differential expression of circRNAs in AMI patients and NCCP controls. (B) Distribution of KEGG Pathway Enrichment for genes matched with exo-circRNA sequences showing differential expression. (C) Five up-regulated circRNAs in AMI selected for the first validation cohort. AMI stands for acute myocardial infarction, and NCCP refers to non-cardiogenic chest pain. exo-circRNA, exosomal circular RNA; KEGG, kyoto encyclopedia of genes and genomes; RPM, reads per million mapped reads.

in the expression of hsa\_circ\_0003270 between patients with acute myocardial infarction (AMI) and those with non-cardiac chest pain (NCCP). However, the detection results for hsa\_circ\_0001535, hsa\_circ\_0000972, and hsa\_circ\_0001558 were consistent with the sequencing results. Specifically, the relative amount of hsa\_circ\_0001535 in the plasma exosomes of AMI patients (8.49 (5.34, 13.94)) was significantly higher than that in the NCCP group (5.45 (3.50, 7.57)) ( $p < 0.05$ ), indicating a 1.56-fold increase in the AMI group (Fig. 4A). Fig. 4B depicts that the calculated area under the Receiver Operating Characteristic (ROC) curve for diagnosing AMI in this cohort is 0.685.

Furthermore, the relative expression level of hsa\_circ\_0000972 in patients with acute myocardial infarction (22.17 (15.73, 32.66)) was significantly higher than that observed in the non-cardiac chest pain group (12.40 (3.43, 25.08)) ( $p < 0.05$ ), indicating a 1.79-fold increase in the acute myocardial infarction cohort. The ROC curve's area for diagnosing AMI in this group was found to be 0.683 (Fig. 4C,D). In comparison, the plasma exosomes of AMI patients exhibited a considerably higher relative expression level of hsa\_circ\_0001558 (27.62 (20.47, 44.81)) compared to the NCCP group (7.42 (4.21, 31.08)) ( $p < 0.01$ ), indicating a 3.72-fold increase in the AMI group. The calculated value for the area under the ROC curve in diagnosing AMI within this group was 0.790, as shown in Fig. 4E,F. Given that hsa\_circ\_0001558 demonstrated the highest area under the ROC curve for diagnosing AMI among these three circRNAs, it was selected for further validation using a larger sample size cohort.

### 3.6 The Second Validation Cohort to Confirm the Exosomal CircRNAs Obtained in the First Validation Cohort

To validate the exosomal circRNAs identified in the initial validation group, we conducted a larger sample validation with 85 AMI patients and 48 NCCP patients, focusing on hsa\_circ\_0001558. For insights into their clinical characteristics, please refer to Table 1 in our previously published data [12]. The demographic characteristics between the two groups were largely evenly distributed.

The findings from the second validation cohort of AMI and NCCP patients demonstrated similar results for the validation of plasma exosomal hsa\_circ\_0001558 as the first validation cohort. The exosomal hsa\_circ\_0001558 in the plasma of AMI patients (8.81 (4.87, 17.76)) exhibited a significantly higher relative expression level compared to the NCCP group (1.98 (0.74, 6.44)), showing a substantial disparity ( $p < 0.01$ ), with the AMI group having a 4.45-fold increase compared to the NCCP group (Fig. 5A). Fig. 5B shows that the ROC curve for diagnosing AMI had an area of 0.793.

Additionally, patients with AMI were categorized into two groups: ST-segment elevation myocardial infarction (STEMI) and non-ST-segment elevation myocardial infarction (NSTEMI). The NSTEMI group exhibited a significantly higher relative expression of plasma exosomal hsa\_circ\_0001558 (5.54 (4.00, 11.96)) compared to the NCCP group (1.98 (0.74, 6.44)), with a 2.80-fold increase in NSTEMI compared to the NCCP group (Fig. 5C). The ROC curve's area under the curve (AUC) for the diagnosis of NSTEMI was 0.72 (Fig. 5D). The STEMI group exhibited a 5.27-fold increase in the relative expression of

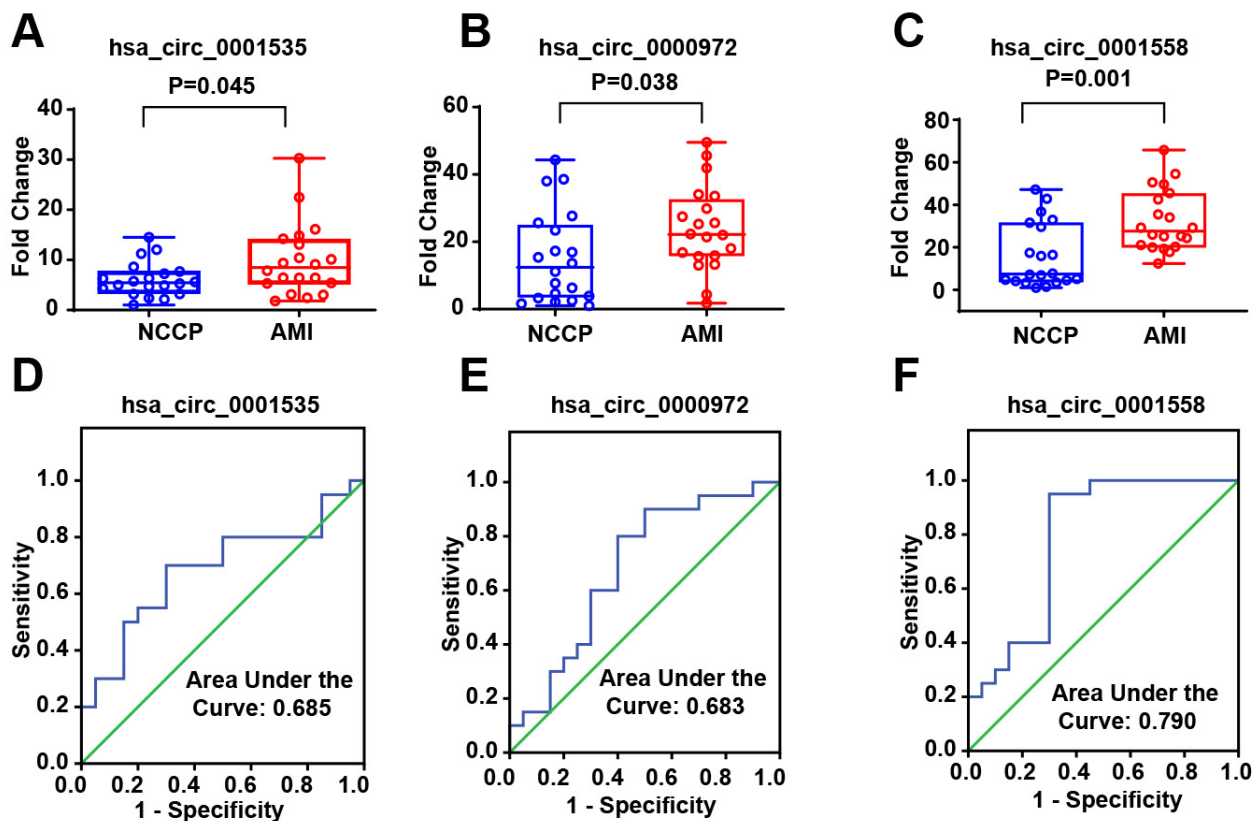


**Fig. 4. Validation results with the first validation cohort.** (A–C) Relative expression levels of hsa\_circ\_0001535 (A), hsa\_circ\_0000972 (B) and hsa\_circ\_0001558 (C) in AMI and NCCP. (D–F) ROC curves of hsa\_circ\_0001535 (D), hsa\_circ\_0000972 (E) and hsa\_circ\_0001558 (F) for diagnosing AMI. ROC, receiver operating characteristic.

plasma exosomal hsa\_circ\_0001558 (10.44 (6.95, 22.93)) compared to the NCCP group and 1.88-fold increase compared to the NSTEMI group (Fig. 5C). Additionally, the area under the ROC curve demonstrated a value of 0.831 for diagnosing STEMI (Fig. 5E) and a value of 0.687 for differentiating STEMI from NSTEMI (Fig. 5F).

#### 4. Discussion

In this study, we conducted a comprehensive examination of the profiles of circulating exosomal circRNAs in patients with acute myocardial infarction (AMI). Among AMI patients, a significant number of circRNAs with differential expression were identified. Genes associated with these circRNAs were enriched in crucial KEGG pathways, indicating their direct relevance to AMI pathophysiology. Furthermore, we validated the expression levels of specific circRNAs, including hsa\_circ\_0001535, hsa\_circ\_0000972, and hsa\_circ\_0001558. Importantly, hsa\_circ\_0001558 emerged as a promising biomarker with substantial diagnostic significance for AMI, as evidenced by the area under the ROC curve.

Analysis of the information substances present in exosomes provides valuable insights into the fundamental characteristics of cells [15,16]. Previous research has mainly

focused on investigating the role and function of miRNA in exosomes, particularly in early AMI detection, transplantation treatment, and the development of myocardial fibrosis and angiogenesis after AMI [17–19]. However, circRNA has recently emerged as a significant information substance within exosomes [20,21]. Numerous studies have demonstrated the involvement of exosomal circRNA in the progression of various illnesses, suggesting its potential as a unique indicator for diagnosing diseases and evaluating prognosis [22,23]. Therefore, exploring the expression patterns of circRNA in exosomes can illuminate the intercellular information exchange processes underlying disease progression. Surprisingly, to date, no literature reports have explored the expression alterations of exosomal circRNA in AMI patients or its potential as a biomarker for AMI.

Initially, through high-throughput sequencing, we observed notable variations in the expression patterns of circRNAs in plasma exosomes from AMI patients compared to the control group. Using the criteria of  $|\log_2(\text{Fold change})| > 1$  and  $q\text{-value} < 0.001$ , we identified 893 circRNAs with differential expression in plasma exosomes from AMI patients. Among these, 118 circRNAs were up-regulated, while 775 were downregulated. These findings

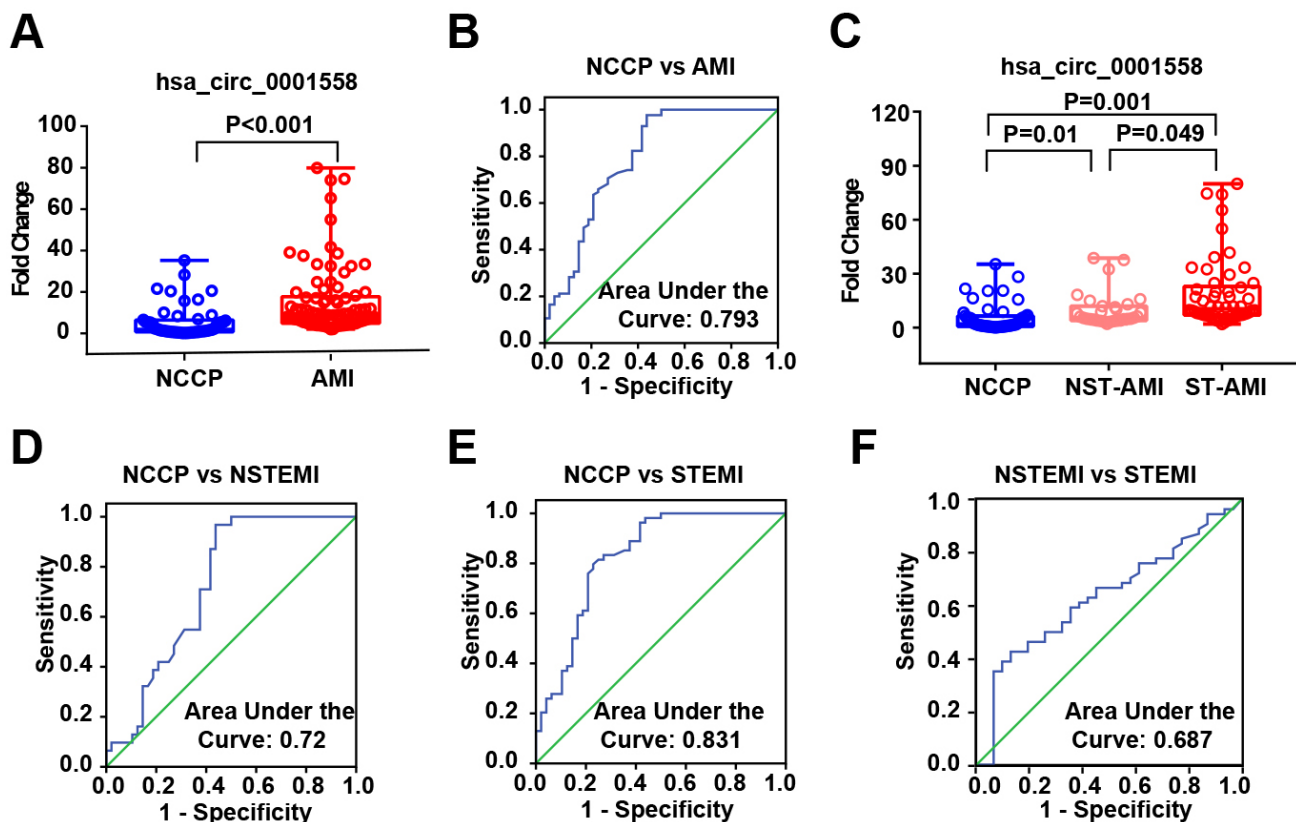


**Fig. 5. Validation results with the second validation cohort.** (A) Expression Levels of hsa\_circ\_0001558 in the plasma exosomes of NCCP and AMI Patients. (B) ROC Curve for the diagnosis of AMI by plasma exosomal hsa\_circ\_0001558. (C) Expression Levels of hsa\_circ\_0001558 in the plasma exosomes of NCCP, NSTEMI, and STEMI Patients. (D,E) ROC Curve for the diagnosis of NSTEMI (D) and STEMI (E) by plasma exosomal hsa\_circ\_0001558. (F) ROC curve for discriminating STEMI from NSTEMI by plasma exosomal hsa\_circ\_0001558. NSTEMI, non-ST-segment elevation myocardial infarction; STEMI, ST-segment elevation myocardial infarction.

suggest that circRNAs are selectively packaged by circulating exosomes during AMI, indicating their potential as biomarkers for AMI.

The inclusion of KEGG pathway analysis in our study regarding genes linked to differentially expressed circRNAs provides new opportunities to comprehend their functional significance in AMI. The significant enrichment of genes in pathways such as focal adhesion, mTOR signaling, cancer pathways, and thyroid hormone signaling suggests a broader biological role for these circRNAs. This enrichment in diverse but crucial pathways underscores the potential of circRNAs in modulating key cellular processes and disease mechanisms. Specifically, their participation in focal adhesion and mTOR signaling pathways corresponds to crucial mechanisms of cell adhesion and growth, playing a vital role in the pathogenesis of AMI [24]. The association with cancer pathways and thyroid hormone signaling also hints at a complex regulatory network influenced by these circRNAs. These insights not only contribute to our understanding of circRNA functions in AMI but also pave the way for future investigations into their potential as therapeutic targets.

We chose five exosomal circRNAs from circBase, considering their annotations, high expression levels, and notable fold changes. Subsequently, we validated them using RT-PCR in a limited sample size. The results affirmed the sequencing findings for hsa\_circ\_0001535, hsa\_circ\_0000972, and hsa\_circ\_0001558. Notably, hsa\_circ\_0001558 exhibited the most significant increase in the AMI group and yielded the highest area under the receiver operating characteristic curve for AMI diagnosis. Consequently, we further validated hsa\_circ\_0001558 in a larger sample size.

The validation outcomes for exosomal hsa\_circ\_0001558 in a larger patient group concurred with the small sample size validation. Its expression in plasma exosomes of AMI patients was significantly higher (4.45-fold increase) compared to the NCCP group. The AUC for AMI diagnosis was 0.793. These findings build on Liu *et al.*'s study [25] identifying exosomal microRNA-4516, microRNA-203, and SFRP1 as potential AMI indicators.

AMI, based on electrocardiographic features, is classified as STEMI and NSTEMI. We subsequently analyzed exosomal hsa\_circ\_0001558 levels in a substantial sample

of STEMI and NSTEMI patients. Results showed a progressive increase in *hsa\_circ\_0001558* expression within plasma exosomes across NCCP, STEMI, and NSTEMI groups. The AUC for diagnosing NSTEMI was 0.72, while for diagnosing STEMI, it was 0.831. Huang *et al.*'s study [26] further underscores the importance of exosomal circRNAs in obstructive sleep apnea patients with AMI, aligning with our identification.

*Hsa\_circ\_0001558* is situated on chromosome 5 and spans 397 nucleotides. It can be detected in various tissues/cells such as platelets, K562 cells, and vascular endothelial cells [27–29]. At present, there is a lack of literature documenting its involvement in physiological/pathological conditions, and additional research is needed to explore its impact on the onset and progression of AMI.

This study's most notable academic achievement is the elucidation of a novel circRNA profile associated with AMI, enriching the circRNA database and providing a new avenue for understanding the molecular mechanisms underlying AMI. The identification and validation of *hsa\_circ\_0001558*, in particular, contribute to the field by offering a promising biomarker for AMI diagnosis. This work demonstrates the clinical potential of circRNAs as biomarkers and affirms the necessity of exosomal analysis in the liquid biopsy landscape, positioning our study as a stepping-stone for future personalized medicine approaches.

Despite the promising findings, this study is not without limitations. The sample size, while adequate for preliminary analysis, warrants expansion in future studies to ensure the generalizability of our results across diverse populations. Furthermore, the functional responsibilities of the identified circRNAs are yet to be clarified, requiring additional investigation to comprehend their biological consequences in the pathophysiology of AMI. Future investigations should also focus on the integration of circRNA profiles with other omics data to establish a more comprehensive biomarker panel for AMI diagnosis and prognosis.

## 5. Conclusions

To sum up, the circRNA expression pattern in exosomes circulating in individuals with AMI differs significantly when compared to the control group. Genes linked to these circRNAs were enriched in crucial KEGG pathways, highlighting their direct relevance to AMI pathophysiology. Moreover, the exosomal *hsa\_circ\_0001558* expression level progressively rises in plasma exosomes of the non-cardiac chest pain (NCCP), STEMI, and NSTEMI groups, suggesting its potential as a diagnostic biomarker for AMI.

## Abbreviations

AMI, acute myocardial infarction; circRNA, circular RNAs; RT-PCR, real-time polymerase chain re-

action; NCCP, non-cardiac chest pain; PBS, phosphate buffer saline; TEM, transmission electron microscopy; PVDF, polyvinylidene fluoride; BSA, bovine serum albumin; CD63, cluster of differentiation 63; NTA, nanoparticle tracking analysis; TEM, transmission electron microscopy; STEMI, ST-segment elevation myocardial infarction; NSTEMI, non-ST-segment elevation myocardial infarction.

## Availability of Data and Materials

Sequence data are available on the Gene Expression Omnibus (GEO; accession number: GSE246758). Other data presented in this study are available upon request from the corresponding author.

## Author Contributions

XL, YZ, XY, BX, and MZ designed the research study. XL, YZ, WY, RH, BX and JZ contributed to the methodology. BX, WY, XL, RH and YZ performed the research. XL, YZ, WY, and MZ analyzed the data. XL, YZ, MZ and WY wrote the manuscript. All authors contributed to editorial changes in the manuscript. JZ, XY and BX revised the manuscript. All authors read and approved the final manuscript. All authors have participated sufficiently in the work and agreed to be accountable for all aspects of the work.

## Ethics Approval and Consent to Participate

The study was conducted in accordance with the Declaration of Helsinki, and approved by the Ethics Committee of Beijing Chaoyang Hospital, Capital Medical University (protocol code 2016-ke-101; Approval Date: 13 July 2016). All participants provided consent after receiving pertinent information.

## Acknowledgment

Not applicable.

## Funding

This research was funded by the General Program of the National Natural Science Foundation of China (No. 82170302), the 2024 Reform and Development Program of Beijing Institute of Respiratory Medicine, the Beijing Natural Science Foundation (No. 7222068), and the Clinical Research Incubation Program of Beijing Chaoyang Hospital Affiliated to Capital Medical University (CYFH202209).

## Conflict of Interest

The authors declare no conflict of interest.

## References

- [1] Wang Y, He L, Du D, Cheng Z, Qin C. A Metabolomics-Based Study on NMDAR-Mediated Mitochondrial Damage through Calcium Overload and ROS Accumulation in Myocardial In-

- farction. *Frontiers in Bioscience (Landmark Edition)*. 2023; 28: 140.
- [2] Krychtiuk KA, Newby LK. High-Sensitivity Cardiac Troponin Assays: Ready for Prime Time! *Annual Review of Medicine*. 2024; 75: 459–474.
  - [3] Cui T, Feng C, Jiang H, Jin Y, Feng J. Inhibition of *PFKFB3* Expression Stimulates Macrophage-Mediated Lymphangiogenesis Post-Acute Myocardial Infarction. *Frontiers in Bioscience (Landmark Edition)*. 2023; 28: 277.
  - [4] Hosseini M, Sahebi R, Aghasizadeh M, Yazdi DF, Salaribaghoonabad R, Godsi A, *et al.* Investigating the predictive value of microRNA21 as a biomarker in induced myocardial infarction animal model. *Gene Reports*. 2022; 27: 101578.
  - [5] Zadeh FJ, Ghasemi Y, Bagheri S, Maleknia M, Davari N, Rezaeeyan H. Do exosomes play role in cardiovascular disease development in hematological malignancy? *Molecular Biology Reports*. 2020; 47: 5487–5493.
  - [6] Altıntaş Ö, Saylan Y. Exploring the Versatility of Exosomes: A Review on Isolation, Characterization, Detection Methods, and Diverse Applications. *Analytical Chemistry*. 2023; 95: 16029–16048.
  - [7] Feng XY, Zhu SX, Pu KJ, Huang HJ, Chen YQ, Wang WT. New insight into circRNAs: characterization, strategies, and biomedical applications. *Experimental Hematology & Oncology*. 2023; 12: 91.
  - [8] Xu J, Ji L, Liang Y, Wan Z, Zheng W, Song X, *et al.* CircRNA-SORE mediates sorafenib resistance in hepatocellular carcinoma by stabilizing YBX1. *Signal Transduction and Targeted Therapy*. 2020; 5: 298.
  - [9] Niu D, Wu Y, Lian J. Circular RNA vaccine in disease prevention and treatment. *Signal Transduction and Targeted Therapy*. 2023; 8: 341.
  - [10] Han C, Yang J, Sun J, Qin G. Extracellular vesicles in cardiovascular disease: Biological functions and therapeutic implications. *Pharmacology and Therapeutics*. 2022; 233: 108025.
  - [11] Li L, Li W, Chen N, Zhao H, Xu G, Zhao Y, *et al.* *FLII* Exonic Circular RNAs as a Novel Oncogenic Driver to Promote Tumor Metastasis in Small Cell Lung Cancer. *Clinical Cancer Research: an Official Journal of the American Association for Cancer Research*. 2019; 25: 1302–1317.
  - [12] Zheng ML, Liu XY, Han RJ, Yuan W, Sun K, Zhong JC, *et al.* Circulating exosomal long non-coding RNAs in patients with acute myocardial infarction. *Journal of Cellular and Molecular Medicine*. 2020; 24: 9388–9396.
  - [13] Qian DY, Yan GB, Bai B, Chen Y, Zhang SJ, Yao YC, *et al.* Differential circRNA expression profiles during the BMP2-induced osteogenic differentiation of MC3T3-E1 cells. *Biomedicine & Pharmacotherapy = Biomedecine & Pharmacotherapie*. 2017; 90: 492–499.
  - [14] Sun X, Wan X, Khan MA, Zhang K, Yi X, Wang Z, *et al.* Comprehensive Analysis of circRNA Expression Profiles in Human Brown Adipose Tissue. *Diabetes, Metabolic Syndrome and Obesity: Targets and Therapy*. 2023; 16: 469–478.
  - [15] Han QF, Li WJ, Hu KS, Gao J, Zhai WL, Yang JH, *et al.* Exosome biogenesis: machinery, regulation, and therapeutic implications in cancer. *Molecular Cancer*. 2022; 21: 207.
  - [16] Cai PY, Zheng YL, Zhou YF, Wang WD, Li MM, Shi YC, *et al.* Research progress on the role of exosomes in obstructive sleep apnea-hypopnea syndrome-related atherosclerosis. *Sleep Medicine Reviews*. 2022; 66: 101696.
  - [17] Park HJ, Hoffman JR, Brown ME, Bheri S, Brazhkina O, Son YH, *et al.* Knockdown of deleterious miRNA in progenitor cell-derived small extracellular vesicles enhances tissue repair in myocardial infarction. *Science Advances*. 2023; 9: eabo4616.
  - [18] Pu Y, Li C, Qi X, Xu R, Dong L, Jiang Y, *et al.* Extracellular Vesicles from NMN Preconditioned Mesenchymal Stem Cells Ameliorated Myocardial Infarction via miR-210-3p Promoted Angiogenesis. *Stem Cell Reviews and Reports*. 2023; 19: 1051–1066.
  - [19] Saenz-Pipaon G, Dichek DA. Targeting and delivery of microRNA-targeting antisense oligonucleotides in cardiovascular diseases. *Atherosclerosis*. 2023; 374: 44–54.
  - [20] Shelton M, Anene CA, Nsengimana J, Roberts W, Newton-Bishop J, Boyne JR. The role of CAF derived exosomal microRNAs in the tumour microenvironment of melanoma. *Biochimica et Biophysica Acta. Reviews on Cancer*. 2021; 1875: 188456.
  - [21] Zhou B, Mo Z, Lai G, Chen X, Li R, Wu R, *et al.* Targeting tumor exosomal circular RNA cSERPINE2 suppresses breast cancer progression by modulating MALT1-NF- $\kappa$ B-IL-6 axis of tumor-associated macrophages. *Journal of Experimental & Clinical Cancer Research: CR*. 2023; 42: 48.
  - [22] Chen C, Liu Y, Liu L, Si C, Xu Y, Wu X, *et al.* Exosomal circ-TUBGCP4 promotes vascular endothelial cell tipping and colorectal cancer metastasis by activating Akt signaling pathway. *Journal of Experimental & Clinical Cancer Research: CR*. 2023; 42: 46.
  - [23] Deng Q, Chen Y, Lin L, Lin J, Wang H, Qiu Y, *et al.* Exosomal hsa\_circRNA\_047733 integrated with clinical features for preoperative prediction of lymph node metastasis risk in oral squamous cell carcinoma. *Journal of Oral Pathology & Medicine: Official Publication of the International Association of Oral Pathologists and the American Academy of Oral Pathology*. 2023; 52: 37–46.
  - [24] Feng L, Li B, Xi Y, Cai M, Tian Z. Aerobic exercise and resistance exercise alleviate skeletal muscle atrophy through IGF-1/IGF-1R-PI3K/Akt pathway in mice with myocardial infarction. *American Journal of Physiology. Cell Physiology*. 2022; 322: C164–C176.
  - [25] Liu P, Wang S, Li K, Yang Y, Man Y, Du F, *et al.* Exosomal microRNA 4516, microRNA 203 and SFRP1 are potential biomarkers of acute myocardial infarction. *Molecular Medicine Reports*. 2023; 27: 124.
  - [26] Huang JF, Lian NF, Lin GF, Xie HS, Wang BY, Chen GP, *et al.* Expression alteration of serum exosomal circular RNAs in obstructive sleep apnea patients with acute myocardial infarction. *BMC Medical Genomics*. 2023; 16: 50.
  - [27] Salzman J, Chen RE, Olsen MN, Wang PL, Brown PO. Cell-type specific features of circular RNA expression. *PLoS Genetics*. 2013; 9: e1003777.
  - [28] Rybak-Wolf A, Stottmeister C, Glažar P, Jens M, Pino N, Giusti S, *et al.* Circular RNAs in the Mammalian Brain Are Highly Abundant, Conserved, and Dynamically Expressed. *Molecular Cell*. 2015; 58: 870–885.
  - [29] Memczak S, Jens M, Elefsinioti A, Torti F, Krueger J, Rybak A, *et al.* Circular RNAs are a large class of animal RNAs with regulatory potency. *Nature*. 2013; 495: 333–338.